Appl. Phys. B (2017) 123:133
DOI 10.1007/s00340-017-6710-2

Applied Physics B
Lasers and Optics

Study on stimulated Raman scattering and up-conversion phenomenon in impure $KGd(WO_4)_2$ crystal

Xiaoqiang Gao[1] · Meng Chen[1]

Received: 29 September 2016 / Accepted: 29 March 2017 / Published online: 7 April 2017

Abstract In order to enhance the efficiency and the output average power of the synchronously pumped stimulated Raman scattering (SRS) system, we studied a picosecond pulse-train synchronously pumped SRS system experimentally. A compact $KGd(WO_4)_2$ (KGW) Raman cavity was synchronously pumped by high average power picosecond pulse-train laser. 1.22 W including eight-order Stokes Raman components were obtained and the maximum Raman conversion efficiency was 35.4% which was the highest efficiency for all-solid-state picosecond synchronously pumped SRS system to our best knowledge. And the "parasitical SRS process" under SRS process in synchronously pumping condition was observed for the first time.

1 Introduction

High order Stokes laser generation by stimulated Raman scattering attracts increasing attention for developing multi-wavelength laser involved applications such as color holography and laser display. Generally, in order to produce orders of Stokes laser as much as possible, improving the pump energy was the most effective method. Usually this method will introduce thermal lens effect or even damage to the laser material (crystal and coating) especially for ultrashort pulse pump condition. In order to improve the high average power picosecond pumped SRS performance, we studied a compact KGW crystal SRS system which was synchronously pumped by a high average power picosecond laser experimentally.

A 50 mm long $KGd(WO_4)_2$ crystal was synchronously pumped by the pump laser via extra-cavity pump technique. Finally, we got up to average power of 1.22 W laser including eight-order Stokes Raman components. The output was also coaxial which was different from former research [1–3] and the maximum Raman conversion efficiency was 35.4%. Furthermore, we have also observed the up-conversion phenomenon. We owe this phenomenon to the combination of high average power pump and small quantity of Er^{3+} ion adoption in the Raman crystal. The cascaded SRS phenomenon ("parasitical SRS process") by the laser ("parasitical light") resulted from the up-conversion process was also observed and analyzed.

Generally, stimulated Raman scattering is a powerful tool to expand the variety of the laser wavelength both in continuous wave [4, 5] generation and ultrashort laser source formation [6] based on the convenient commercial laser devices. Recently, the system which can provide multi-wavelengths at the same time is highly needed for improving system compatibility in order to employ to much more applications, such as coherent anti-Stokes Raman scattering (2D-CARS) thermometry system [7]. In order to get broader range of wavelengths covered, we have to increase the average power of the input, which leads to thermal loading [8] problems due to impurity of the Raman medium. Furthermore, the impure Raman crystal which has trace of adoption not only absorbs the pump laser which result in thermal effect, but also can absorbs the Stokes laser and radiates laser which generally in form of up-conversion [9, 10]. Due to high power pump, parasitical light via up-conversion can stimulate the Raman crystal to generate other Stokes components. This process (parasitical

✉ Meng Chen
chenmeng@bjut.edu.cn

Xiaoqiang Gao
xqgao@emails.bjut.edu.cn

[1] Beijing University of Technology, Beijing 100124, China

SRS process) parasitizes under the SRS process while no report has been published to describe it in detail.

In this paper, we reported a high average power eight-order Stokes Raman laser experimentally in experiment section and the parasitical SRS process has also been discussed in detail in discussion part.

2 Experiment setup

Figure 1 illustrates the setup for pulse-train picosecond laser pumped Raman system, which comprises pulse-train pump laser [11], polarization modulation elements, KGW crystal Raman cavity, and the analysis devices.

The pump laser has pulse-train profile with repetition frequency of 1 kHz and ~30 ps pulse width (FWHM) for every pulse in the "train," and every train has 6 pulses separated by 800 ps delay time. The input mirror was coated high transparency ($R < 0.5\%$) for 532 nm and high reflective ($R > 99.8\%$) for longer wavelength (up to 1000 nm) with a -200 mm radius of curvature. The output coupler was configured as a concave lens ($r = -500$ mm) with transmission rate of 5% for the wavelength from 500 to 800 nm.

As excellent crystalline Raman medium, KGW crystal has much more advantages compared with other Raman crystals especially for picosecond pump condition [12]. The high gain (3.3 cm/GW for 901 cm^{-1}) of Raman makes it suitable for high power Raman laser generation and the wide transmission range (0.35–5.5 um) indicates the widely usage for producing broad-band laser, what is more, the short dephase time (4–5 ps) [13] appeals ultrashort Raman laser researches. Furthermore, when doped with lanthanide ions, the crystal becomes excellent laser medium cite [14, 15].

In our experiment, we utilized a b-cut 7 mm × 7 mm × 50 mm KGW crystal (provided by EKSMA) as Raman medium which coated high transparency ($T > 99.8\%$) for the range of 500–900 nm for both ends of the crystal. In order to maintain the crystal thermal loading ability, we packaged it into an aluminum sink which was cooled continuously with water at a temperature of 23 °C.

At the beginning of the experiment, the pump laser was attuned by a tunable attenuator, which comprises thin film polarizer (TFP) and half-wave plate (HWP), and then propagated through a quarter-wave plate (QWP). The QWP precisely modulated the pump polarization in order to make the pump perfectly match the Raman mode of the KGW crystal. Generally, the pump was focused into Raman crystal to get high Raman gain [16], while in our experiment, the pump was collimated into the Raman cavity without focusing for the following reasons: the parallel light decreases the possibility of four-wave-mixing (FWM) process which will degenerate orientation consistency of the output laser for avoiding introducing the angle for phase

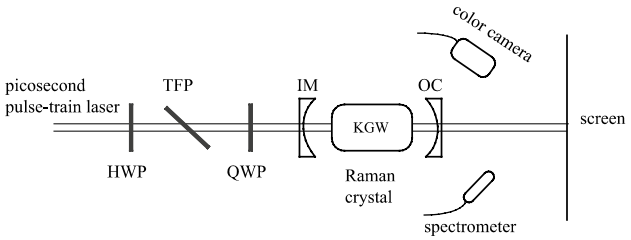

Fig. 1 Setup for pulse-train synchronously pumped Raman experiment (*HWP* half-wave-plate, *QWP* quarter-wave-plate, *TFP* thin film polarizer, *IM* input mirror, *OC* output coupler)

matching in FWM process. Furthermore, the collimated input laser will make it convenient to design a simple structured Raman cavity for without considering the resonant mode changes induced by focused input laser, and the most important advantage is that the parallel light decreases the risk of the damage for both crystal and cavity mirror especially for high average power pump system which was the first consideration for commercial use both in intra-cavity or extra-cavity configuration SRS system.

After propagating through the Raman cavity, the output laser power characteristics was measured by power meter (Ophir) and the spectroscopy was observed by fiber coupled spectrometer (ocean optics USB2000+) and analyzed by computer software (Spectrasuit, ocean optics), the beam profile was recorded by color camera and near infrared (NIR) camera.

3 Results and discussion

The output laser contains Stokes components without any anti-Stokes which means that the process was pure cascaded stimulated Raman scattering (SRS) without four-wave-mixing (FWM) process which generally was the only way to generate anti-Stokes components. The first-Stokes laser threshold is 300 mW and is almost the other higher order Stokes components' thresholds except the eighth Stokes. The threshold for 8th order Stokes laser is about 1.06 W higher than threshold of the other higher order Stokes components for crystal coating transmittance (<20%) limitation. Figure 2 plots the output spectroscopy when the pump power was 1.4 W. The amplitude of the spectra expresses the real strength of the Raman components for without inserting any attenuator between spectrometer and the reflected laser.

It is notable that the amplitudes of 532 nm, first-Stokes, second-Stokes, third-Stokes, and fourth-Stokes are almost the same level which indicates effective Raman conversion from fundamental to Stokes. The visible output laser components are shown by Fig. 3a; the radius of the laser beam for different color were not the

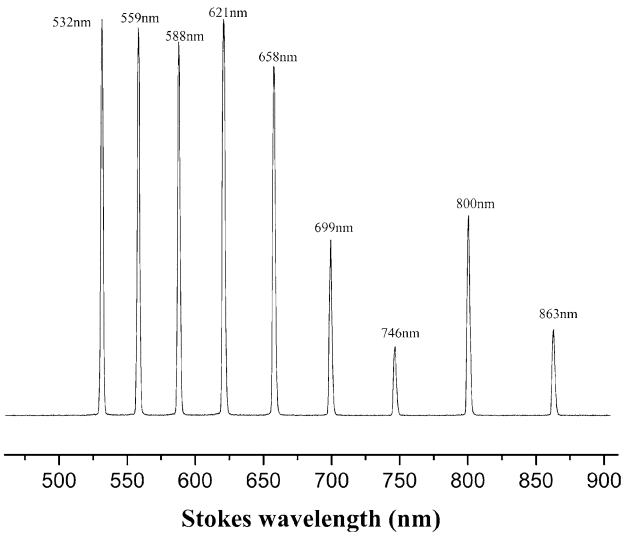

Fig. 2 Output spectroscopy of Raman cavity pumped by average power of 1.4 W

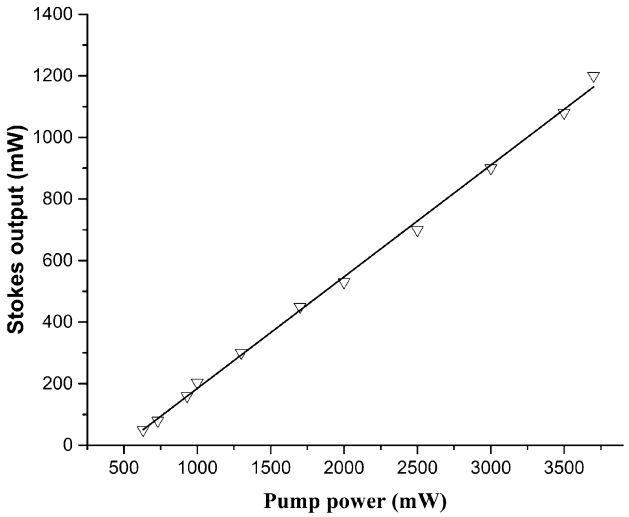

Fig. 4 Output power under different pump

same due to dispersion existing in the Raman crystal. In order to observe much more wavelengths, the laser beam was split by a grating and the diffracted components were recorded by NIR camera which was capable to capture both visible and NIR band light as grayscale image (Fig. 3b).

When increasing the pump power, the higher order Stokes light has not been observed due to the crystal coating high reflective rate (>90%).

The output power versus input power was illustrated by Fig. 4:

Table 1 shows the individual output power for each Stokes line:

Finally, we got up to 1.02 W eight Stokes light with Raman conversion of 35.4%, overall efficiency of 42.4% and with slope efficiency of 36.3%. When the pump was higher than 3.6 W, the ninth Stokes laser and the first anti-Stokes laser existed, and up-conversion phenomenon accompanied with the parasitical SRS process was observed through spectrometer (Fig. 5a). Figure 5b illustrates the relative strength of the Stokes light and the parasitical Stokes light.

The first anti-Stokes laser indicates that the FWM process appeared in the crystal. The phase matching condition was provided from lens-like effect (or thermal lens effect) of the crystal due to absorption of the pump. The phenomenon mentioned above certified the existence of adoption in Raman crystal. Under high average power pump condition, the adoption ion in the Raman crystal can absorb the pump laser and Raman components which depends on the absorption characteristics of the type of the adoption.

In our experiment, the parasitical light components contain: 527, 554, 584, 617, 652, 660, 696, 743, 798, and 860 nm, the light components correspond to 527 nm and its SRS Stokes spectroscopy at 901 cm^{-1} Raman mode. We owe the parasitical Stokes light of 527 nm to the impurity of the Raman crystal KGW, which are resulted

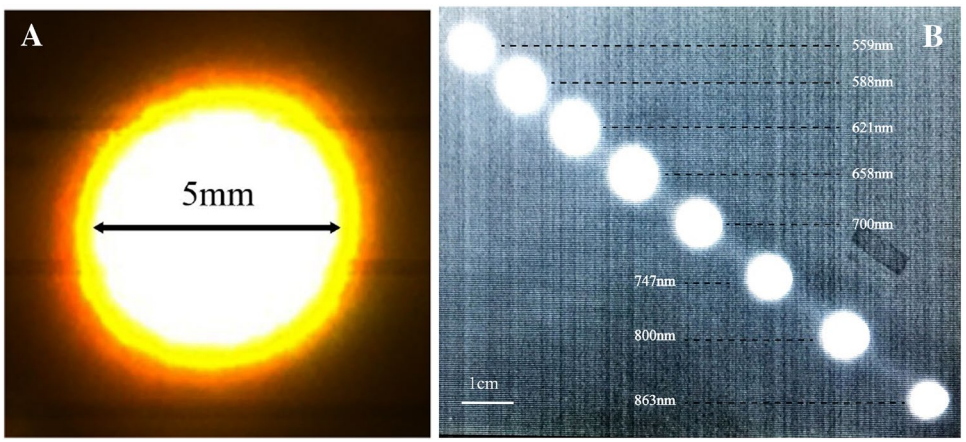

Fig. 3 Beam profile of the output, **a** beam profile of the visible part, **b** beam profiles after split by a grating

Table 1 Output power for Stokes components

Wavelength/nm	532 nm	559 nm	589 nm	621 nm	657 nm	699 nm	746 nm	800 nm	864 nm
Power/mW	197.9	189.8	186.7	194.9	174.9	90.0	37.7	102.0	46.1
Line width/nm	0.20	0.24	0.22	0.23	0.22	0.23	0.21	0.22	0.20

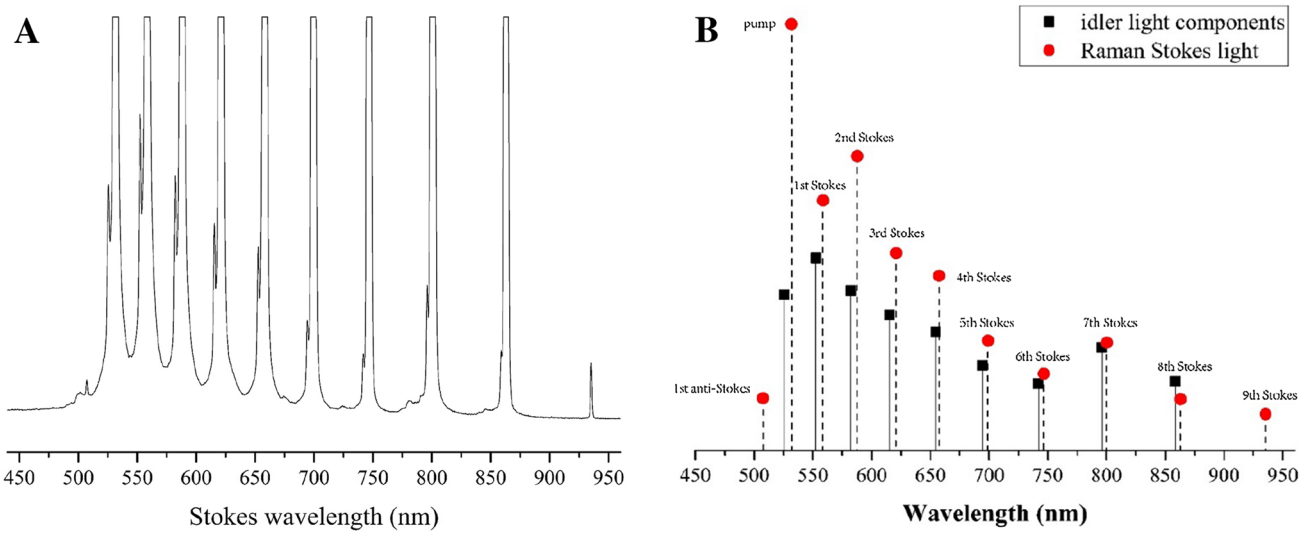

Fig. 5 **a** SRS spectroscopy with parasitical Stokes light, **b** Idler light and Stokes components (the Stokes components was decayed by a ratio of 0.3)

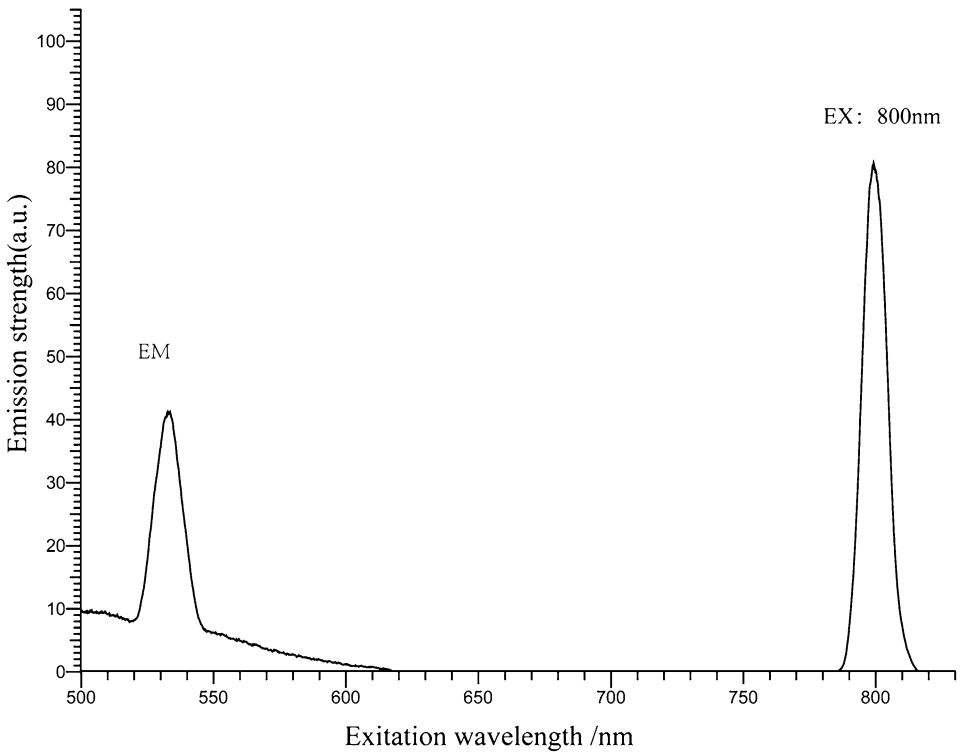

Fig. 6 Fluorescence spectroscopy profile for the crystal used in experiment

from Er^{3+} doping due to imperfection of the crystal growth technique. Compared with the wavelength of the pump, the process of producing 527 nm laser was up-conversion process. The following describes the up-conversion process and the relative parasitical SRS process in our Raman cavity:

After cascaded SRS process excited by 532 nm, the Er^{3+} ion doped in the Raman crystal can absorb the Raman Stokes components, which depends on the absorption peak of Er^{3+} ions (800 nm, 7th Stokes) [17], and the emission happened between Energy state of $^2H_{11/2}$ and $^4I_{15/2}$, with a radiation of 527 nm. Then the strong emission of 527 nm (which was called "parasitical light") stimulated the Raman crystal and the another SRS process (which was called "parasitical SRS process") happened under the SRS process which was activated by 532 nm pump laser. The Stokes light stimulated by parasitical light was called as "parasitical Stokes light." We examined the same crystal used in our experiment using Fluorescence spectrometer (Hitachi-F7000 fluorescence spectrometer), Fig. 6 illustrates the results for excitation wavelength (EX) and emission wavelength (EM).

The excitation laser covers 520–545 nm, which is also the excitation wavelength region of Er^{3+} [18] proving the existence of the Er^{3+} ion.

4 Conclusion

We demonstrated an efficient Raman laser which produced up to 1.22 W pulse-train collinear eight Stokes Raman laser. The up-conversion phenomenon was observed in our experiment. The up-conversion process has been reported for many times [9, 19, 20], while the cascaded SRS process due to this phenomenon was the first report to our best knowledge. Due to up-conversion and its cascaded SRS process, the output wavelength has been broadened and the spectroscopy components also have been enriched. However, the linear absorption due to up-conversion decreases the Raman conversion which should be avoided in much higher pump condition.

References

1. P.G. Zverev, J.T. Murray, R.C. Powell, R.J. Reeves, T.T. Basiev, Stimulated Raman scattering of picosecond pulses in barium nitrate crystals. Opt. Commun. **97**, 59 (1993)
2. P.G. Zverev, T.T. Basiev, A.M. Prokhorov, Stimulated Raman scattering of laser radiation in Raman crystals. Opt. Mater. **11**, 335–352 (1999)
3. W. Wei, X.Y. Zhang, Q.P. Wang, Theoretical and experimental study on intracavity pumped $SrWO_4$ anti-Stokes Raman laser. Appl. Phys. B Lasers Opt. **116**(3), 561–568 (2014)
4. X. Li, Multiwavelength visible laser based on the stimulated Raman scattering effect and beta barium borate angle tuning. Chin. Opt. Lett. **14**(2), 021404 (2016)
5. J. Jakutis-Neto, J. Lin, N.U. Wetter, H. Pask, Continuous-wave watt-level Nd:YLF/KGW Raman laser operating at near-ir, yellow and lime-green wavelengths. Opt. Express **20**(9), 9841–9850 (2012)
6. J.T. Murray, W.L. Austin, R.C. Powell, Intracavity Raman conversion and Raman beam cleanup. Opt. Mater. **11**, 353–371 (1999)
7. J.D. Miller, M.N. Slipchenko, J.G. Mance, S. Roy, J.R. Gord, H.U. Stauffer, Burst-mode two-dimensional coherent anti-Stokes Raman scattering (2D-cars) at 1 khz, in *Imaging and Applied Optics 2016*, *LW5G.5*. (Optical Society of America, 2016)
8. A. McKay, O. Kitzler, R.P. Mildren, Thermal lens evolution and compensation in a high power KGW Raman laser. Opt. Express **22**(6), 6707–6718 (2014)
9. D.K. Mohanty, V.K. Rai, Y. Dwivedi, S.B. Rai, Enhancement of up conversion intensity in Er^{3+} doped tellurite glass in presence of Yb^{3+}. Appl. Phys. B **104**(1), 233–236 (2011)
10. K. Mishra, Y. Dwivedi, S.B. Rai, Observation of avalanche up conversion emission in $Pr:Y_2O_3$ nanocrystals on excitation with 532 nm radiation. Appl. Phys. B **106**(1), 101–105 (2012)
11. X.Q. Gao, M.L. Long, M. Chen, Compact $KGd(WO_4)_2$ picosecond pulse-train synchronously pumped broad-band Raman laser. Appl. Opt. **55**, 6554–6558 (2016)
12. D.J. Spence, E. Granados, H.M. Pask, R.P. Mildren. KGW and diamond picosecond visible Raman lasers, in *Lasers*, *Sources and Related Photonic Devices* (Optical Society of America, 2010), p. ATuA20
13. I.V. Mochalov, Laser and nonlinear properties of the potassium gadolinium tungstate laser crystal $KGd(WO_4)_2:Nd^{3+}$-(KGW:Nd). Opt. Eng. **36**(6), 1660–1669 (1997)
14. T. Graf, J.E. Balmer, Lasing properties of diode-laser-pumped Nd:KGW. Opt. Eng. **34**(8), 2349–2352 (1995)
15. A.A. Kaminskii, P.V. Klevtsov, L. Li, A.A. Pavlyuk, Stimulated emission from $KY(WO_4)_2$: Nd^{3+} crystal laser. Phys. Status Solidi (a) **5**(2), K79–K81 (1971)
16. R.T. Mildren, M. Convery, H.M. Pask, J.A. Piper, Efficient, all-solid-state, Raman laser in yellow, orange and red. Opt. Express **12**(5), 785–790 (2004)
17. M.C. Pujol, M. Rico, C. Zaldo, R. Sole, V. Nikolov, X. Solans, M. Aguilo, F. Diaz, Crystalline structure and optical spectroscopy of Era^{+}-doped $KGd(WO_4)_2$ single crystals. Appl. Phys. B **68**(2), 187–197 (1999)
18. W.A. Pisarski, J. Pisarska, R. Lisiecki, Ł. Grobelny, G. Dominiak-Dzik, W. Ryba-Romanowski, Luminescence spectroscopy of rare earth-doped oxychloride lead borate glasses. J. Lumin. **131**(4), 649–652 (2011)
19. Xu Wei, Zhiguo Zhang, Wenwu Cao, Excellent optical thermometry based on short-wavelength upconversion emissions in Era^{+}/Yb^{3+} codoped $CAWO_4$. Opt. Lett. **37**(23), 4865–4867 (2012)
20. B.I. Denker, B.I. Galagan, S.E. Sverchkov, Up conversion losses in different erbium-doped laser glasses. Appl. Phys. B **120**(2), 367–372 (2015)